



# Fermilab

## An Estimate of the Longitudinal Coupling Impedance of the Energy Doubler

King-Yuen Ng

May 1981

### I. Introduction

In this note, we try to estimate the longitudinal coupling impedance for the Energy Doubler, which is essential for the stability of a particle beam. We find that the longitudinal coupling impedance per unit harmonics  $|Z_n/n|$  starts off with ~50 ohms which is due to the resistivity of the beampipe and the resistivity of the laminations of the Lambertsons. It falls off as  $n^{-1/2}$  and when the harmonic  $n \gtrsim 10^2$ , it is lower than a few ohms both at injection (150 GeV/c<sup>2</sup>) and ejection (1000 GeV/c<sup>2</sup>) energies.

Our discussion follows closely that of Faltens and Laslett<sup>1</sup> and Ruggiero<sup>2</sup>.

Before estimating the longitudinal impedances, let us first get an idea how much can be reasonably allowed. We take as a stability criterion, the Keil-Schnell formula

$$\left| \frac{Z_n}{n} \right| \leq \frac{|\eta|E}{eI_p} \left( \frac{\Delta E}{E} \right)^2, \quad (1.1)$$

where  $\eta$  is the momentum compaction factor of the accelerator,  $E$  the energy,  $\Delta E$  the FWHM energy spread and  $e$  the proton charge. Equation (1.1) is derived for a coasting beam. However, it can be applied to a bunched beam provided that  $I_p$  is interpreted as the instantaneous peak current in a bunch which is related to the average current  $I_{AV}$  by

$$I_p = I_{AV} \frac{\sqrt{2\pi R}}{3M\sigma_\ell}$$

where  $R$  is the average radius of the accelerator ring and there are  $M$  bunches each of r.m.s. length  $\sigma_\ell$ . Also, the following two criterions have to be satisfied:

$$\text{wave length of instability } (\lambda = \frac{2\pi R}{n}) \ll \text{ bunch length ,} \quad (1.2)$$

$$\text{growth time of instability} \ll \text{ period of synchrotron oscillation.} \quad (1.3)$$

For the Energy Doubler, we take

$$R = 10^5 \text{ cm ,}$$

$$\eta = 0.0028 ,$$

$$M \sim 1000 ,$$

$$I_{AV} = 0.15 \text{ amp } (2 \times 10^{13} \text{ ppp}) ,$$

$$\text{RF harmonic } h = 1113 ,$$

and obtain

$$\sigma_\ell = 140 S^{1/2} E^{-1/4} V_{RF}^{-1/4} \text{ cm ,}$$

$$\frac{\Delta E}{E} = 0.026 S^{1/2} E^{-1/4} V_{RF}^{1/2} \text{ cm ,}$$

with the RF voltage  $V_{RF}$  in MV,  $E$  in GeV and the invariant bunch area  $S$  in eV-sec.

Using  $V_{RF} = 2.16$  MV and  $S = 0.3$  eV-sec, we find that criterions (1.2) and (1.3) are satisfied when the harmonic of instability is  $n \geq 5 \times 10^4$ . Thus from Eq. (1.1),

$$\left| \frac{Z_n}{n} \right| < \begin{cases} 34 \text{ ohms} & \text{at } 150 \text{ GeV/c} \\ 8.1 \text{ ohms} & \text{at } 1000 \text{ GeV/c}^2. \end{cases} \quad (1.4)$$

Therefore, when  $n \geq 5 \times 10^4$ , our estimation shows that the bunched beam is stable.

The following sections are devoted to free-space radiation, space-charge

and wall resistance, impedance due to curvature of beampipe, bellows, monitor-plates, steps in vacuum chamber, RF cavities, sniffers and Lambertsons. Finally a summary is given.

## II. Free-space radiation

Without any beampipe, in free space, the power spectrum radiated by a particle carrying charge  $e$  and travelling along a curve with radius of curvature  $\rho$ , as derived by Schwinger<sup>3</sup>, is

$$P(\omega, t) = \frac{1}{3^{\frac{1}{6}}} \frac{\Gamma(\frac{2}{3}) e^2}{\pi \rho} \left(\frac{\omega}{\omega_0}\right)^{\frac{1}{3}} \left\{ 1 - \frac{\Gamma(\frac{2}{3})}{2} \left(\frac{\omega}{2\omega_c}\right)^{\frac{1}{3}} + \dots \right\} \quad (2.1)$$

for  $\omega \ll \omega_c$ , and drops exponentially as

$$P(\omega, t) = \frac{3}{4} \left(\frac{3}{2\pi}\right)^{\frac{1}{2}} \frac{e^2}{\rho} \gamma^4 \left(\frac{\omega_0}{\omega_c}\right) \left(\frac{\omega}{\omega_c}\right)^{\frac{1}{2}} e^{-\frac{\omega}{\omega_c}} \left\{ 1 + \frac{55 \omega_c}{72 \omega} + \dots \right\} \quad (2.2)$$

when  $\omega \gg \omega_c$ . In above, the instantaneous angular frequency  $\omega_0$  is defined as

$\omega_0 = \beta c / \rho$ , the critical angular frequency is  $\omega_c = \frac{3}{2} \gamma^3 \omega_0$

$\beta$  and  $\gamma$  are the relativistic parameters of the charge particle. The coupling impedance  $R_n$  at the  $n$ th harmonic ( $n \equiv \frac{R\omega}{\beta c}$  and  $R$  = average radius of accelerator ring) can be obtained from  $P_n$ , the power radiated into the  $n$ th harmonic, by  $R_n = 2P_n / I_n^2$ , where  $I_n = e\beta c / \pi R$  for  $n \neq 0$  is the  $n$ th harmonic Fourier current amplitude of a  $\delta$ -function charge travelling in the accelerator ring. Inclusion of the reactive terms<sup>4</sup> leads to the impedance

$$\frac{Z_n}{n} = 354 n^{-\frac{2}{3}} \left(\frac{\sqrt{3}}{2} + j \frac{1}{2}\right) \quad (2.3)$$

when  $\omega \ll \omega_c$ , where we have set  $\rho = R$ . For the Doubler,  $R = 10^5$  cm but  $\rho = 7.54 \times 10^4$  cm for the part with dipole magnets. This modifies Eq. (5) to

$$\frac{Z_n}{n} = 322 n^{-\frac{2}{3}} \left(\frac{\sqrt{3}}{2} + j \frac{1}{2}\right). \quad (2.4)$$

Although Eq. (2.4) is within the stability limit of Keil-Schnell for  $n > 5 \times 10^4$ , we are not sure whether it is too high at low harmonics, where the stability criterion is still unclear. However, our beam is placed inside a beampipe of radius  $b \sim 3.5$  cm. As a result, below the cutoff harmonic  $n_{\text{cutoff}} = \frac{R}{b} (2.405) = 6.9 \times 10^4$  (for TM mode), the beam particles cannot radiate at all and thus the impedance is lowered. Starting from  $n_{\text{cutoff}}$ , the beam particles radiate reaching the free-space value of  $\sim .1 \Omega$  shortly afterwards<sup>1</sup>. The radiation is completely absorbed by the beampipe and is a real loss. In reality, due to the various discontinuities placed along the beampipe, the cutoff frequency is reduced and the beam particles start radiating earlier. Although the beam particles are forbidden to radiate at low frequencies, we need to pay the price of having extra impedances due to the beampipe, which we will discuss in the following sections.

### III. Impedances due to space-charge and wall resistance

The space-charge impedance and resistive wall impedance for an infinitely long straight cylindrical beam pipe are well-known. If we let  $a$  = beam size radius,  $b$  = beam pipe radius and  $X = n/R\gamma$ , then when  $Xb \ll 1$

$$Z_n/n = - \frac{jZ_0}{\beta\gamma^2} \left( \frac{1}{2} + \ln \frac{b}{a} \right) + \frac{1}{\sqrt{2}b} (1+j) \sqrt{\frac{\beta Z_0 R}{n\sigma}}, \quad (3.1)$$

when  $Xb \gg 1$  but  $Xa \ll 1$

$$Z_n/n = - \frac{jZ_0}{\beta\gamma^2} \left( \ln \frac{2\gamma R}{na} - .327 \right), \quad (3.2)$$

and when  $Xa \gg 1$

$$Z_n/n = - \frac{2jZ_0 R^2}{\beta n^2 a^2} \left( 1 - \frac{\gamma R}{na} \right) + (1-j) \frac{2}{a^3} \left( \frac{Z_0^3 \sigma R^7}{\beta^5 n^7} \right)^{\frac{1}{2}} \quad (3.3)$$

where  $\sigma$  is the conductivity of the pipe wall and  $Z_0 = 120 \pi$  ohms is the free-space impedance. The emittance of the beam in the main ring is  $\epsilon = 1.5 \pi$  mm-mrad at  $\sim 8.9$  GeV/c<sup>2</sup> and is inversely proportional to the beam energy.

The  $\beta$ -oscillation parameter for the Doubler has a maximum of  $\beta_{\max} \sim 100$  m, so that the beam size radius is

$$a = \begin{cases} .30 \text{ cm} & \text{at } 150 \text{ GeV}/c^2, \\ .12 \text{ cm} & \text{at } 1000 \text{ GeV}/c^2. \end{cases} \quad (3.4)$$

The beam pipe is made of stainless steel having a conductivity of  $13.7 \times 10^3 \text{ mho-cm}^{-1}$ . The space-charge and resistive wall impedances are plotted in Figs. 1 and 2 along with the free-space radiation impedance (solid curve is the real part and dashed curve is the imaginary part). We note that, at low harmonics, they are much lower than the free-space radiation value and change from inductive to capacitive at high harmonics.

#### IV. Impedance due to curvature of beam pipe

In reality, the beam pipe curves around to form a toroid. When the harmonic is high enough and the particle velocity is sufficiently close to  $c$ , the beam harmonic wave can match an excited wave in angular velocity around the toroid giving a resonance<sup>1</sup>.

For a beam pipe of rectangular cross section of height  $h$  and width  $2b$ , the resonant wave has a vertical electric field proportional to

$$Z(r) = J_n(qR_-)N_n(qr) - J_n(qr)N_n(qR_-) \quad (4.1)$$

for the TM mode (in the vertical sense) and a vertical magnetic field proportional to

$$\tilde{Z}(r) = J_n'(qR_-)N_n(qr) - J_n(qr)N_n'(qR_-) \quad (4.2)$$

for the TE mode, where  $J_n$ ,  $N_n$  are Bessel and Neumann functions of order  $n$ ,

$$R_{\pm} = R(1 \pm \frac{b}{R})$$

are the major outer and inner radii of the toroidal ring, and

$$q^2 = \frac{n^2 \beta^2}{R^2} - \frac{(2k+1)^2 \pi^2}{h^2}$$

with  $k = 0, 1, 2, \dots$ . The corresponding resonant harmonics are obtained by solving for  $n$  from

$$Z(R_+) = 0 \quad \text{TM} \quad (4.3)$$

$$\tilde{Z}'(R_+) = 0 \quad \text{TE} . \quad (4.4)$$

Taking  $b \sim h/2 \sim 3.1$  cm (the size of the square beampipe of the dipoles), the resonant harmonics for the Energy Doubler are computed both at extraction energy and injection energy and are tabulated in Tables 1 and 2. We note, in particular, the lowest modes

$$n_{\text{res}} = \begin{cases} 9.9 \times 10^6 & \text{at injection} \\ 3.4 \times 10^7 & \text{at injection} \end{cases}$$

which are in the TE mode. The figure of merit is roughly given by

$$Q \sim \frac{2}{\delta} \frac{\text{volume}}{\text{surface}} = \frac{b}{\delta}$$

where  $\delta = \sqrt{2R/nZ_0\sigma}$  is the skin depth and  $\sigma$  the wall conductivity. For these modes,

$$Q = \begin{cases} 4.9 \times 10^4 & \text{at extraction} \\ 9.2 \times 10^4 & \text{at injection} . \end{cases}$$

The shunt impedance at resonance is given by

$$\left(\frac{Z_n}{n}\right)_{\text{res}} = \frac{4\pi^3 Z_0 Q}{n^2 q^2} \frac{R^2}{h^3 b} (2k+1)^2 \frac{|Z(x)|_{\text{beam}}^2}{\int_{-1}^1 dx (1 + \frac{bx}{R}) Z^2(x)} \quad (4.5)$$

for the TM mode and\*

\*In Ref. 2, the corresponding formula is in error by having an extra power of  $n$  in the denominator; so the result there might have been underestimated by several orders of magnitude.

$$\left(\frac{Z_n}{n}\right)_{\text{res}} = \frac{4\pi Z_0 Q}{n^2 q^2} \frac{R^2}{hb^3} \frac{\left|\frac{d\tilde{Z}(x)}{dx}\right|_{\text{beam}}^2}{\int_{-1}^1 dx \left(1 + \frac{bx}{R}\right) \tilde{Z}^2(x)} \quad (4.6)$$

for the TE mode, where the radial distance from the vertical axis of symmetry of the ring has been rewritten as

$$r = R\left(1 + \frac{b}{R}x\right).$$

The lowest TE and TM modes are found to have shunt impedances per harmonic of

$$\left(\frac{Z_n}{n}\right)_{\text{res}} = \begin{cases} 9.0 \times 10^{-3} \Omega & \text{TE} \\ 1.4 \times 10^{-3} \Omega & \text{TM} \end{cases}$$

at extraction energy, and

$$\left(\frac{Z_n}{n}\right)_{\text{res}} = \begin{cases} 1.2 \times 10^{-4} \Omega & \text{TE} \\ 3.8 \times 10^{-6} \Omega & \text{TM} \end{cases}$$

at injection energy. Note that for respectively TE and TM modes, for large  $k$

$$\left(\frac{Z_n}{n}\right)_{\text{res}} \propto n^{-\frac{7}{2}}, \quad n^{-\frac{3}{2}}.$$

Thus the impedance per harmonic drops extremely fast after the first few resonances (see Figs. 1 and 2). Also a small change in  $n$  will lead to big changes in  $\left(\frac{Z_n}{n}\right)_{\text{res}}$  if the error in  $n$  is not due to errors in  $b$  and  $h$ .

The lowest modes are summarized in the following:

E	$n_{\text{res}}$	Q	$\left(\frac{Z_n}{n}\right)_{\text{res}}$
150 GeV/c <sup>2</sup>	$3.4 \times 10^7$	$9.2 \times 10^4$	$1.2 \times 10^{-4} \Omega$
1000 GeV/c <sup>2</sup>	$9.9 \times 10^6$	$4.9 \times 10^4$	$9.0 \times 10^{-3} \Omega$

In reality, the beam has a radial spread; the beam particles travel with

different velocities at different radial distances and thus give resonances at different positions. For particles at a radial distance  $R+\Delta R$ , the change of velocity is given by

$$\frac{\Delta\beta}{\beta} = \frac{\gamma_T^2}{\gamma^2} \frac{\Delta R}{R}$$

with  $\gamma_T$  related to the momentum compaction factor by  $\eta = \gamma_T^{-2} - \gamma^{-2}$ . Thus the fields excited at the center of the beampipe have a change of velocity given by

$$\begin{aligned} \frac{\Delta\beta}{\beta} &= \left( \frac{\gamma_T^2}{\gamma^2} - 1 \right) \frac{\Delta R}{R} = -\gamma_T^2 \eta \frac{\Delta R}{R} \\ &\sim - \frac{\Delta R}{R} \end{aligned} \quad (4.7)$$

in our case where the beam energy is much bigger than the transition energy. Faltens and Laslett<sup>1</sup> had given a formula for the harmonic  $n$  of the lowest resonance that could be excited by a beam travelling at the center of a circular beampipe of radius  $b$ :

$$\beta\left(1+\frac{b}{R}\right) = 1 + 0.80862 n^{\frac{2}{3}}. \quad (4.8)$$

Note that this formula leads to a resonance at different harmonic from our former calculation when the square beampipe is approximated as circular. Nevertheless, with Eq. (4.8), when the resonant harmonic is changed by unity, the change in velocity of the fields excited at the center is

$$\Delta\beta\left(1+\frac{b}{R}\right) = -\frac{2}{3} \times 0.80862 n^{-\frac{5}{3}}$$

and the corresponding displacement of the beam from the center is

$$\begin{aligned} \Delta R &\cong \frac{2}{3} \times 0.80862 n^{-\frac{5}{3}} R \\ &= \begin{cases} 1.5 \times 10^{-8} \text{ cm} & \text{at injection energy} \\ 1.2 \times 10^{-7} \text{ cm} & \text{at extraction energy.} \end{cases} \end{aligned}$$

This is just the radial spacing of the beam particles in the beampipe for successive azimuthal resonances (each differs by unity). Taking into account

their high Q's, the resulting shunt impedances should be about one hundred times larger. However, the components of the beam current at such high harmonics are extremely small. As a result, the power lost to these resonances may turn out to be negligible.

#### V. Bellows

The dipoles, quads, spool-pieces and beam pipes are joined together by bellows. There are roughly one thousand bellows each of maximum length  $\ell = 4.68$  cm and average radius  $d = 4.26$  cm. They are joined to beam pipe of radius  $b = 3.49$  cm.

Here

$$\frac{2\pi R}{\ell} = 1.34 \times 10^5 \gg 1 ,$$

$$\frac{R}{\beta d} = 2.35 \times 10^4 \gg 1 , \quad (5.1)$$

with  $R$  = average radius of the accelerator ring and  $\beta$  the velocity of the beam particles. According to Keil and Zotter,<sup>5</sup> for harmonics  $n \ll \frac{R}{\beta d}$  and  $\frac{2\pi R}{\ell}$ , the impedance per harmonic per bellow seen by the beam is

$$\frac{Z_n}{n} = jZ_0 \beta \frac{\ell}{2\pi R} \ln \frac{d}{b} = j(5.57 \times 10^{-4}) \Omega \quad (5.2)$$

where  $Z_0 = 120 \pi$  ohms is the characteristic impedance of free space. In above, the convolutions of the bellow as well as the resistivity of the wall have been neglected.

For one thousand bellows, we have

$$\frac{Z_n}{n} = j(.56) \text{ ohms.} \quad (5.3)$$

In reality, the wall of the bellow has resistivity and the image current has to flow around each convolution. There are, on the average, 24 convolutions in each bellow. Each convolution has an amplitude or depth

$\tau = 0.635$  cm. Thus the image current travels a distance of  $\sim 2\tau$  for each convolution, and the impedance is

$$Z_{\omega} = \frac{2\tau}{2\pi d} \mathcal{R} \quad (5.4)$$

and for 1000 bellows or 24,000 convolutions, the impedance per harmonic is

$$\frac{Z_n}{n} = \frac{Z_{\omega}}{n} (24,000) \sim \frac{0.42}{\sqrt{n}} (1+j). \quad (5.5)$$

In above  $\mathcal{R} = (1+j)\rho/\delta$  is the surface resistivity of the wall,  $\delta$  is the skin depth, and  $\rho$  is the resistivity of the wall taken to be  $73 \times 10^{-6}$  ohm-cm for stainless steel.

At higher frequencies, the convolutions will exhibit resonances. We approximate the convolutions by rectangular wiggles as in Fig. 3. The gap is given by

$$\Delta \sim \frac{\lambda}{2 \times 24} \sim .0976 \text{ cm.} \quad (5.6)$$

Each gap can now be viewed as a transmission line for which we assign a capacitance per unit length and an inductance per unit length

$$C = \frac{\epsilon_0 2\pi d}{\Delta} \text{ and } L = \frac{\mu_0 \Delta}{2\pi d} \quad (5.7)$$

respectively. The input impedance for this line is

$$Z_i = Z_c \tanh \sqrt{yz} \tau, \quad (5.8)$$

where the characteristic impedance of the line is

$$Z_c = \sqrt{\frac{z}{y}}, \quad (5.9)$$

the series impedance per unit length is

$$z = j\omega L + Z_{\omega}/\tau \quad (5.10)$$

and the shunt admittance per unit length is

$$y = j\omega C. \quad (5.11)$$

The resistive impedance of the line  $Z_\omega$  is given by Eq. (5.4) and  $\omega$  is the angular frequency of the electromagnetic fields.

The  $k$ th resonance occurs when  $\tan \text{Im}\sqrt{yz} \tau = \infty$ , or on neglecting  $Z_\omega$ ,

$$\begin{aligned} n_k &= \frac{\pi}{2} (2k-1) \frac{R}{\tau B} \quad k = 1, 2, \dots \\ &= (2.47 \times 10^5)(2k-1). \end{aligned} \quad (5.12)$$

When  $n \ll 2.47 \times 10^5$ , the input impedance is  $Z_i = z\tau$ , leading to a longitudinal impedance per harmonic due to convolutions alone

$$\frac{z_n}{n} = j(.21) + (1+j) \frac{.42}{\sqrt{n}} \text{ ohms.} \quad (5.13)$$

At resonances, the shunt impedance per line is

$$\begin{aligned} Z_i &= Z_C \coth \text{Re} \sqrt{yz} \tau \\ &\sim \frac{2Z_C^2}{Z_\omega}. \end{aligned} \quad (5.14)$$

If all the 24,000 convolutions resonance at exactly the same harmonics, the shunt impedance per harmonic becomes

$$\frac{z_n}{n} = \frac{Z_i}{n} \times 24,000 = \frac{42.9}{(2k-1)^{3/2}} \text{ ohms} \quad (5.15)$$

which is outside the limit for stability, Eq. (1.4). The figure of merit of the resonances is

$$Q_k = \frac{\Delta}{\delta} = 242\sqrt{2k-1}. \quad (5.16)$$

If the amplitude  $\tau$  of the convolutions has a statistical spread of  $\pm\bar{\Delta}$ , the resonant frequencies of the 24,000 convolutions will have a spread of  $\pm 2\bar{\Delta}n_k/\tau$ . In this case, the shunt impedance will be lowered by a factor

$$S_k = \frac{\tan^{-1} \frac{2\bar{\Delta}}{\tau} Q_k}{\frac{2\bar{\Delta}}{\tau} Q_k} . \quad (5.17)$$

For example,  $2\bar{\Delta}/\tau \sim 10\%$  will lead to shunt impedance per harmonics

$$\frac{Z_n}{n} = \frac{2.71}{(2k-1)^{3/2}} \Omega , \quad (5.18)$$

which is still rather high. Since  $Z_n/n \propto \tau^{3/2}$ , the impedance per harmonic can be reduced by using bellows with a smaller convolution amplitude. Also shorter bellows will help too. The contribution of bellows is plotted in Fig. 4.

## VI. Monitor-plates

In each quad, there is a pair of plates monitoring the beam. Each plate is of length  $\ell = 18$  cm subtending an angle  $2\phi_0$  at the beam axis, and is terminated at both ends by a resistance which equals the characteristic impedance  $Z_0$  of the plate with the beam pipe. For  $M$  plates, the longitudinal coupling impedance<sup>6</sup> seen by the beam is

$$Z_L = M \left( \frac{\phi_0}{\pi} \right)^2 Z_C \left[ \frac{2}{qa} \frac{I_1(qa)}{I_0^2(qb)} \right] (1 - \cos 2\phi \cos 2\theta - j \cos 2\theta \sin 2\phi), \quad (6.1)$$

where

$$q = n/R\gamma ,$$

$$2\theta = n\ell/R ,$$

$$2\phi = n\ell\beta/R ,$$

$a$  is the beam radius,  $b$  is the beam pipe radius,  $\beta$  and  $\gamma$  are the relativistic parameters of the beam particles and  $I_i$  is the  $i$ th order modified Bessel function. When  $\gamma \gg 1$ , the last factor of Eq. (6.1) becomes

$$j(\sin 2\theta - \theta\gamma^{-2} \cos 2\theta)e^{-j2\theta} . \quad (6.2)$$

Thus  $Z_L$  starts from zero at  $n = 0$ , becomes inductive and changes to capacitive at  $n = \pi R/2\ell$ . It is clear from Eq. (6.2) that there is no resonance at all frequencies. The geometrical factor

$$\frac{2}{qa} \frac{I_1(qa)}{I_0^2(qa)} \sim 1$$

when  $qb \ll 1$  and falls exponentially when  $qb \gg 1$ . The transition takes place at

$$n_c \sim \frac{\gamma R}{b} = \begin{cases} 4.30 \times 10^6 & \text{at } \gamma = 150, \\ 2.87 \times 10^7 & \text{at } \gamma = 1000. \end{cases} \quad (6.3)$$

Before this critical harmonic is reached, Eq. (6.1) can be written as (assuming that  $\gamma \gg 1$ )

$$Z_L = jM \left(\frac{\phi_0}{\pi}\right)^2 Z_C \sin \frac{n\ell}{R} e^{-jn\ell/R}. \quad (6.4)$$

Thus

$$|Z_L| < M \left(\frac{\phi_0}{\pi}\right)^2 Z_C, \quad (6.5)$$

and when  $n\ell/R \ll 1$ ,

$$\frac{Z_L}{n} = j \frac{M\ell}{R} \left(\frac{\phi_0}{\pi}\right)^2 Z_C.$$

There are 216 quads; there are two plates in each quad. We assume  $M = 432$ . Thus below  $n_c$ ,

$$|Z_L| < 2020 \text{ ohms}$$

where we have taken  $2\phi_0 = 110^\circ$  and  $Z_C = 50$  ohms. When  $n \ll R/\ell = 5.56 \times 10^3$ ,

$$\frac{Z_L}{n} = j(0.36) \text{ ohms.}$$

Thus the longitudinal impedance per harmonic due to the monitor-plates

is inductive and constant at low harmonics, starts dropping like  $1/n$  and alternating between inductive and capacitive when  $n \geq 5.56 \times 10^3$ . When  $n \geq 4.3 \times 10^6$  at injection energy (or  $2.9 \times 10^7$  at injection energy), it drops exponentially (see Fig. 5).

### VII. Vacuum Chamber Steps

The dipoles, quads and spool-pieces are joined together by bellows; so there are steps in the vacuum chamber. Let

$$S = \frac{d}{b} = \frac{\text{outer radius}}{\text{inner radius}}.$$

According to Hereward,<sup>7</sup> when  $n \leq n_W = \frac{\pi R}{b(S-1)}$ , the impedance per harmonic per step is

$$\frac{Z_n}{n} = (1+j\pi) \frac{2Z_0}{\pi} \frac{b}{2\pi R} (S-1)^2, \quad (7.1)$$

and when  $n > n_W$ ,

$$\frac{Z_n}{n} = \frac{Z_0}{2\pi} \frac{S-1}{n}. \quad (7.2)$$

For bellow joined to beam pipe,  $d = 4.26$  cm and  $b = 3.49$  cm; so  $S = 1.22$ . Thus  $n_W = 4.09 \times 10^5$ . There are about  $\sim 2000$  steps in the Energy Doubler. Therefore when  $n \leq 4.09 \times 10^5$ ,

$$\frac{Z_n}{n} = .42 \exp j 72 \cdot 3^0 \text{ ohms.}$$

and when  $n > 4.09 \times 10^5$ ,

$$\frac{Z_n}{n} = \frac{2.64 \times 10^4}{n},$$

which equals .065 when  $n$  is replaced by  $n_W$ . Thus the contribution of steps to the longitudinal coupling impedance per harmonic is small. The result is plotted in Fig. 6.

## VIII. RF Cavities

The present design of the Doubler includes three RF cavities whose contribution to the longitudinal impedance is to be studied here. When the RF system is loaded with a beam of  $2.5 \times 10^{13}$  ppp, the fundamental mode is characterized by

$$\begin{aligned} \text{resonant harmonic } n_R &= 1113 , \\ \text{figure of merit } Q &= 3650 , \\ \text{shunt impedance } Z_S &= 0.5 \text{ M}\Omega \text{ per cavity} . \end{aligned} \quad (8.1)$$

Because of the high  $Q$ , the cavity is well approximated by a RLC lumped circuit with

$$R = \frac{Z_S}{Q} , \quad L = \frac{Z_S}{Q\omega_R} , \quad \text{and } C = \frac{Q}{\omega_R Z_S} , \quad (8.2)$$

with  $\omega_R$  the resonant angular frequency. Therefore we get for the longitudinal impedance for the  $n$ th harmonic

$$Z_n = \frac{Z_S}{1 + jQ\left(\frac{n}{n_R} - \frac{n_R}{n}\right)} . \quad (8.3)$$

Slightly away from the peak of the resonance, the impedance is reduced to

$$\frac{Z_n}{n} = \frac{Z_S n_R}{4Q^2 (n - n_R)^2} . \quad (8.4)$$

For example,  $|n - n_R| \geq 10$  leads to  $Z_n/n \leq .10$  well within the tolerable range for stability. As a result, large value of  $Z_n/n$  can be avoided by adding RF bypass loops at  $n_R$ .

However, there are still substantial reactive contributions at other frequencies. At frequencies well below  $\omega_R$ , i.e.,  $n \ll n_R$ , from Eq. (5.3),

$$\begin{aligned}\frac{Z_n}{n} &\approx \frac{Z_s}{Q} \frac{n}{n_R^3} + \frac{Z_s}{n_R Q} \\ &= 3.03 \times 10^{-8} n + j(\cdot 12)\end{aligned}\quad (8.5)$$

which is inductive and changes to capacitive well above  $\omega_R$ , i.e.,  $n \gg n_R$ ,

$$\begin{aligned}\frac{Z_n}{n} &\approx \frac{Z_s}{Q} \frac{n_R}{n^3} - j \frac{Z_s}{Q} \frac{n_R}{n^2} \\ &= \frac{41.8}{n^3} - j \frac{1.52 \times 10^5}{n^2},\end{aligned}\quad (8.6)$$

which equals  $3.03 \times 10^{-9} - j(\cdot 12)$  when  $n$  is replaced by  $n_R$ . The fractional errors in Eqs. (8.5) and (8.6) are  $O(n^2/n_R^2)$  and  $O(n_R^2/n^2)$  respectively. For three cavities,  $Z_n/n$  will be three times bigger; however, it is well within the stability limit of Eq. (1.4).

## VI. Sniffers

There are sniffers in spool-pieces. They are circular holes of radius  $a$  in the beam pipe. When half of the wavelength  $\lambda/2$  of the beam wave is very much bigger than the diameter of the hole, the radiation loss can be approximated<sup>8</sup> by Bethe's diffraction.<sup>9</sup> That is, the diffracted field at each hole is approximately the fields coming from an equivalent electric dipole

$$\vec{d} = -\frac{2\epsilon_0}{3} a^3 \vec{E}_0 \quad (9.1)$$

and an equivalent magnetic moment

$$\vec{m} = -\frac{4}{3\mu_0} a^3 \vec{B}_0 \quad (9.2)$$

placed at the hole, where  $\vec{E}_0$  is the electric field and  $\vec{B}_0$  the magnetic field at the position of the hole when the hole is not present. The powers radiated

from the dipole and magnetic moment are respectively

$$P_d = \frac{Z_0 |\ddot{\vec{d}}|^2}{6\pi c^2} \quad (9.3)$$

and

$$P_m = \frac{Z_0 |\ddot{\vec{m}}|^2}{6\pi c^4} \quad (9.4)$$

Now, with the absence of the hole, the electric field perpendicular to the beam pipe and the magnetic field parallel to the beam pipe are respectively

$$|\vec{E}_0| = \frac{I_n}{2\pi b \epsilon_0 \beta c} \quad \text{and} \quad |\vec{B}_0| = \frac{\mu_0 I_n}{2\pi b}, \quad (9.5)$$

where  $I_n$  is the beam current in the nth harmonic,  $\beta c$  is the velocity of the beam particle and  $b$  is the radius of the beam pipe. One half of the power diffracted at the hole is reflected back into the beam pipe and the other half is lost. Thus the total power lost in the nth harmonic is

$$P_n = \frac{5}{108\pi} Z_0 I_n^2 n^4 \frac{a^6 \beta^4}{b^2 R^4}, \quad (9.6)$$

and the longitudinal impedance per harmonic due to one hole is

$$\frac{Z_n}{n} = \frac{5}{54\pi} Z_0 n^3 \frac{a^6 \beta^4}{b^2 R^4}. \quad (9.7)$$

When  $\frac{\lambda}{2} \ll 2a$ , we can use ordinary geometric optics. If the pipe wall is perfectly conducting, a plane wave with magnetic field  $H$  and electric field  $E = Z_0 H$  (all are magnitudes) incident normally on the wall will be reflected as shown in Fig. 7, such that the total magnetic and electric fields at the wall are respectively

$$H_0 = 2H \quad \text{and} \quad E_0 = 0. \quad (9.8)$$

We know that  $H_0 = I_n/2\pi b$ , so

$$H = \frac{E}{Z_0} = \frac{I_n}{4\pi b} \quad (9.9)$$

When a hole is present with diameter much bigger than one half the wavelength of the plane wave, there will be no reflection and the incident wave just passes through the hole and is lost. Thus the power lost in harmonic  $n$  is

$$\begin{aligned} P_n &= \frac{1}{2} \int ds \vec{E} \times \vec{H} = \frac{1}{2} \pi a^2 Z_0 H^2 \\ &= \frac{1}{2} I_n^2 \frac{Z_0}{16\pi} \cdot \frac{a^2}{b^2} \end{aligned} \quad (9.10)$$

and the corresponding longitudinal impedance per harmonic is

$$\frac{Z_n}{n} = \frac{Z_0}{16\pi} \frac{a^2}{b^2} \frac{1}{n} \quad (9.11)$$

In above we have neglected the circumstance that the beam is bunched. This is quite all right because in a proton storage ring, the bunch length is very much bigger than the diameter of the beam pipe.

Numerically, radius of sniffer  $a = 1.93$  cm, radius of beam pipe  $b = 3.49$  cm. The critical harmonic is, therefore,

$$n_c = \frac{\pi R}{2a} = 8.2 \times 10^4 \quad (9.12)$$

There are roughly 250 sniffers. Thus

$$\frac{Z_n}{n} = \begin{cases} 1.16 \times 10^{-16} n^3 \text{ ohms} & \text{when } n \ll n_c \\ \frac{570}{n} = \text{ohms} & \text{when } n \gg n_c \end{cases}$$

which is only  $\sim .07$  when  $n$  is replaced by  $n_c$ . Thus the sniffers offer no

threat to stability at all. The result is plotted in Fig. 6.

### X. Electrostatic Septum

The electrostatic septum consists of a U-shaped block of aluminum of length  $\ell = 600$  cm, width  $\sim 11.5$  cm and gap  $2b = 4.15$  cm, Fig. 8. Except for extraction, the beam is far from the septum wires. So we can approximate the septum by two parallel plates with the beam in the center. The longitudinal impedance per harmonic is

$$\begin{aligned} \frac{Z_n}{n} = -jZ_0 \frac{1}{2\pi R} \frac{1}{\beta\gamma^2} & \left\{ \frac{1}{2} + \int_0^\infty d\eta \tilde{\sigma}_\eta^2 \frac{\tanh \eta b}{n} \right\} \\ & + \frac{2R\ell}{n} \int_0^\infty d\eta \tilde{\sigma}_\eta \operatorname{sech}^2 \eta b, \end{aligned} \quad (10.1)$$

where  $R$  is the surface resistivity,  $\tilde{\sigma}_\eta$  is the cosine transform of the horizontal profile of the beam. For an infinitely narrow beam,  $\tilde{\sigma}_\eta = \frac{1}{2\pi}$ . If it has a narrow width of  $2a$ ,  $\tilde{\sigma}_\eta$  tapers off when  $|\eta| > \pi/2a$ . Using  $\rho = 2.8 \mu\Omega\text{-cm}$  for the resistivity of aluminum,

$$\begin{aligned} \left(\frac{Z_n}{n}\right)_{\text{space charge}} & \cong -jZ_0 \frac{\ell}{2\pi R} \frac{1}{\beta\gamma^2} \left(\frac{3}{2} + \ell n \frac{\pi b}{2a}\right) \\ & = \begin{cases} -j 6.2 \times 10^{-5} \text{ ohms} & \text{for } \gamma = 150 \\ -j 1.73 \times 10^{-6} \text{ ohms} & \text{for } \gamma = 1000 \end{cases} \end{aligned} \quad (10.2)$$

and

$$\left(\frac{Z_n}{n}\right)_{\text{wall}} = \frac{R\ell}{2\pi b n} = \frac{3.34 \times 10^{-3}}{\sqrt{n}} (1+j), \quad (10.3)$$

which are plotted in Fig. 6. These numbers are negligibly small compared with the stability requirement of Eq. (1.4).

### XI. Extraction and Injection Lambertson

There are five extraction Lambertsons each of length 220 in. The beam is very near to the vertex of the field-free region (see Fig. 9a) so that

the image current will concentrate near the vertex too. In order to complete the circuit, this image current has to flow around each lamination of the Lambertsons up to perhaps the stainless steel stiffeners which are approximately 5 cm away. Very roughly, we approximate<sup>10</sup> the Lambertsons by an annular stack of iron laminations of total thickness  $\ell = 5 \times 220$  in., inner radius  $b \sim 3.0$  cm and outer radius  $b+d \sim 8$  cm, and is shorted at the outer circumference (Fig. 9b). The beam is at a distance  $f \sim \frac{3}{8}$  in = .953 cm from a point on the inner circumference. We define an off-center parameter for the beam

$$g = 1 - \frac{f}{b} = .682 . \quad (11.1)$$

Then the longitudinal impedance<sup>10</sup> for the nth harmonic is

$$Z_n = -jZ_0 \frac{n\ell}{2\pi R} \frac{1}{\beta\gamma^2} \left[ \frac{1}{2} + \ell n \left( \frac{b}{a} \cdot \frac{1-g^2}{1+g^2} \right) \right] + \frac{\ell R_{\text{eff}}}{2\pi b} \cdot \frac{1+g^2}{1-g^2} , \quad (11.2)$$

where  $a$  is the beam radius

$$a = \begin{cases} .30 \text{ cm} & \text{at } 150 \text{ GeV}/c^2 , \\ .12 \text{ cm} & \text{at } 1000 \text{ GeV}/c^2 . \end{cases} \quad (11.3)$$

The first term is the space-charge part which gives

$$\left( \frac{Z_n}{n} \right)_{\text{sp.ch.}} = \begin{cases} 1.34 \times 10^{-4} \text{ ohms} & \text{at } 150 \text{ GeV}/c^2 , \\ 4.54 \times 10^{-6} \text{ ohms} & \text{at } 1000 \text{ GeV}/c^2 , \end{cases} \quad (11.4)$$

which is too small to affect stability. The second term is the effective wall resistive part with an effective surface resistivity  $R_{\text{eff}}$  which will take into account the penetration of electromagnetic fields into the lamination gaps.

Each lamination has a thickness  $\tau = .0953$  cm and a gap  $\Delta \sim 3\%$  of  $\tau$  or .00296 cm. Since the image current flows along the edge of each lamination as well as its two surfaces, we have an impedance due to resistivity

$$Z_r = \frac{R\ell}{2\pi b} + \frac{R\ell}{\pi\tau} \ln\left(1 + \frac{d}{b}\right), \quad (11.5)$$

where  $R = (1+j)\rho/\delta$  and  $\rho$  and  $\delta$  are the resistivity and skin depth of the lamination respectively. Due to the path length difference, the second term, the flow along the surfaces is  $\sim 100$  times bigger than the first term, the flow along the edges; so the latter is neglected.

Each gap can be viewed as a radial transmission line shorted at the far end. We can assign an approximate capacitance "per unit length" and an inductance "per unit length"

$$C = \frac{\epsilon_0 \pi d}{\Delta} \left(1 + \frac{2b}{d}\right), \quad L = \frac{\mu_0 \Delta}{2\pi d} \ln\left(1 + \frac{d}{b}\right). \quad (11.6)$$

The input impedance is

$$Z_i = Z_c \tanh \sqrt{yz} d, \quad (11.7)$$

where  $Z_c = \sqrt{z/y}$  is the characteristic impedance of the line and

$$z = j\omega L + \frac{R}{\pi d} \ln\left(1 + \frac{d}{b}\right)$$

and

$$y = j\omega C \quad (11.8)$$

are the series impedance per unit length and shunt admittance per unit length of the line,  $\omega$  being the angular frequency of the field.

The  $k$ th resonance occurs when  $\tan \text{Im}\sqrt{zy} d$  reaches the  $k$ th infinity, i.e., neglecting  $R$ ,

$$\begin{aligned}
 n_k &= \frac{\pi R}{2d} (2k-1) \\
 &= 3.14 \times 10^4 (2k-1) \quad k = 1, 2, 3, \dots
 \end{aligned}
 \tag{11.9}$$

When  $n \ll 3.14 \times 10^4$ ,  $Z_i = zd$ , we get

$$R_{\text{eff}} = \frac{2\pi b}{\tau} \left( \frac{R}{\pi} + \frac{j\omega\mu_0\Delta}{2\pi} \right) \ln\left(1 + \frac{d}{b}\right) .
 \tag{11.10}$$

Thus from Eq. (11.2),

$$\left( \frac{Z_n}{n} \right)_{\text{wall}} = \frac{9.30}{\sqrt{n}} (1+j) + j(0.14) .
 \tag{11.11}$$

This impedance per harmonic is perhaps too high at low  $n$ , where the stability criterion is still unknown for bunched beams.

For the  $k$ th resonance, the figure of merit is

$$Q_k \sim \frac{\Delta}{\delta} = 2.53\sqrt{2k-1} ,
 \tag{11.12}$$

and the shunt impedance per gap is

$$\begin{aligned}
 Z_s &= Z_c \coth \operatorname{Re}\sqrt{yz}d \\
 &\sim Z_0 \frac{\Delta}{2\pi b} \coth \frac{pd}{Z_0\Delta\delta}
 \end{aligned}
 \tag{11.13}$$

giving an effective surface impedance of

$$R_{\text{eff}} = \frac{2\pi b}{\tau} Z_s .
 \tag{11.14}$$

Therefore at the  $k$ th resonance, using Eq. (11.2), the longitudinal impedance per harmonic is

$$\frac{Z_n}{n} = \frac{.28}{(2k-1)^{3/2}} \text{ ohms} . \quad (11.15)$$

Although each gap will not resonate at the same harmonic, the extremely small figure of merit  $Q_k$  implies that the smearing out of the resonances of the various gaps will not lower  $Z_n/n$  at all as is evident from Eq. (5.17).

The situation of the injection Lambertsons is exactly the same. There, we have four Lambertsons each of length 189 in. So we only need to scale the resulting impedances per harmonic by  $\frac{4 \times 189}{5 \times 220}$  giving

$$\left(\frac{Z_n}{n}\right)_{\text{wall}} = \frac{6.39}{\sqrt{n}} (1+j) + j(.10) \text{ ohms} \quad (11.16)$$

when  $n \ll 3.14 \times 10^4$  and

$$\frac{Z_n}{n} = \frac{5.18}{(2k-1)^{3/2}} \text{ ohms} \quad (11.17)$$

as the shunt impedance per harmonic for the  $k$ th resonance. The results are plotted in Fig. 10.

## XII. Abort Lambertsons

In order that the beam can be aborted as fast as possible, the beam is at all times very close to the wall of the abort Lambertsons, Fig. 11a. The space occupied by the beam is rectangular in shape with the width very much bigger than the height. Thus, it can be approximated as two parallel plates separated by a distance  $2b = 4.08$  cm, with the beam at a distance  $f \sim \frac{3}{8}$  in from the upper plate,

The space-charge part of the longitudinal impedance per harmonic is

$$\left(\frac{Z_n}{n}\right)_{\text{sp.ch.}} = -jZ_0 \frac{1}{2\pi R} \frac{1}{\beta\gamma^2} \left\{ \frac{1}{2} + 4\pi^2 \int_0^\infty d\eta \tilde{\sigma}_\eta^2 \times \right. \\ \left. \times \frac{\tanh \eta b}{\eta} \left[ 1 - \frac{\sinh^2 \eta(b-f)}{\sinh^2 \eta b} \right] \right\} \quad (12.1)$$

where  $\ell = 6 \times 490$  cm is the total length of the six abort Lambertsons,  $\tilde{\sigma}_\eta$  is the cosine transform of the transverse beam profile. For a beam width of  $2a \ll 2b$ ,  $\tilde{\sigma}_\eta \sim \frac{1}{2\pi}$  and tapers off when  $|\eta| > \pi/2a$ . This space charge part  $(Z_n/n)_{\text{sp.ch.}}$  is  $\sim 10^{-5} \Omega (10^{-7} \Omega)$  at injection (extraction) energy which is too small to affect stability and can be neglected.

If there are no laminations, the wall effect leads to an impedance

$$Z_n = R\ell/2\pi f, \quad (12.2)$$

when  $f/b \ll 1$ , where  $R = (1+j)\rho/\delta$  is the surface resistivity,  $\rho$  and  $\delta$  are the resistivity and skin depth of the upper wall. This can be interpreted as having an image current flowing in a width of  $2\pi f$  in a depth  $\delta$  with resistivity  $\rho$ , Fig. 11b. Now because of the lamination in reality, this current has to flow around each gap along the surfaces of the laminations. In general, when flowing along the surfaces of the laminations, the current will fan out since the magnetic field fans out when farther away from the beam. But due to the stainless steel stiffeners which are roughly at a distance  $d \sim 5$  cm from the upper wall and where the image current will turn around along the surface of another lamination, it is a good assumption that there is no fanning. Thus the resistive impedance of Eq. (12.2) becomes

$$Z_r = Z_{\text{edge}} + Z_{\text{gap}} \\ = \frac{R\ell}{2\pi f} + \frac{R}{2\pi f} \cdot \frac{\ell}{\tau} \cdot 2d, \quad (12.3)$$

where  $\tau \sim .037$  in. = .0953 cm is the thickness of each lamination and

therefore  $l/\tau$  represents the total number of gaps. Since  $2d/\tau \sim 104 \gg 1$ , the first term can be neglected.

Each gap can be viewed as a parallel - plate transmission line for which the capacitance per unit length and inductance per unit length are respectively

$$C = \frac{\epsilon_0 2\pi f}{\Delta} \quad \text{and} \quad L = \frac{\mu_0 \Delta}{2\pi f}, \quad (12.4)$$

where  $\Delta \sim 3\%$  of  $\tau$  is the gap width. The input impedance of each transmission line is

$$Z_i = Z_C \tanh \sqrt{yz} d, \quad (12.5)$$

where the characteristic impedance is

$$Z_C = \sqrt{z/y}$$

and the series impedance per unit length and shunt admittance per unit length are respectively

$$z = \frac{R}{\pi f} + j\omega L \quad \text{and} \quad y = j\omega C, \quad (12.6)$$

where  $\omega = n\beta c/R$  is the angular frequency of the fields. The  $k$ th resonance occurs at  $\tan \text{Im} \sqrt{yz} d = \infty$  or

$$\begin{aligned} n_k &= (2k-1) \frac{\pi R}{2d} \\ &= 3.4 \times 10^4 (2k-1) \end{aligned} \quad (12.7)$$

where the shift due to resistivity has been neglected. When  $n \ll 3.14 \times 10^4$ ,  $Z_i = zd$ , and for the six Lambertsons,

$$\begin{aligned} \frac{Z_n}{n} &= \left( \frac{2R}{2\pi f} + \frac{j\omega\mu_0 \Delta}{2\pi f} \right) \frac{d}{n} \frac{\ell}{\tau} \\ &= \frac{19.1}{\sqrt{n}} (1+j) + j(.278) \text{ ohms} , \end{aligned} \quad (12.8)$$

which may be too big at low harmonics, where the stability criterion is still unknown for bunched beams.

For the kth resonance, the figure of merit is

$$Q_k \cong \frac{\Delta}{\delta} = 2.53\sqrt{2k-1} \text{ ohms} \quad (12.9)$$

and the shunt impedance per gap is

$$\begin{aligned} Z_{\text{shunt}} &= Z_c \coth \operatorname{Re}\sqrt{yz} d \\ &\sim Z_0 \frac{\Delta}{2\pi f} \coth \frac{\rho d}{Z_0 \Delta \delta} \end{aligned} \quad (12.10)$$

giving for the six Lambertsons,

$$\frac{Z_n}{n} = \frac{.58}{(2k-1)^{3/2}} \text{ ohms} . \quad (12.11)$$

There are  $3.09 \times 10^4$  gaps and there will be  $3.09 \times 10^4$  resonances at the fundamental mode. Although they will spread out in frequency, the smallness of  $Q_k$  will not lower the shunt impedance at all. As a result, it may be necessary to install copper foil at the upper wall so as to screen off the laminations and lower the longitudinal impedance to a value safer for stability. The result is plotted in Fig. 12.

### XIII. Summary

All the contributions discussed above are added up in Figs. 13 and 14 for injection energy and extraction energy respectively. The contribution

due to RF cavities have not been included because there is not enough information for the parasitic modes as well as their damping mechanism. Also the effects of the kickers magnets have not been included because their final design is not available. The two figures are very similar. The real part starts off with  $Z_n/n \sim 50 n^{-1/2}$  ohms with contribution mainly from the resistive walls of the beampipe and the resistive surfaces of the laminations in the Lambertsons. Just below  $n \sim 10^4$ , the contributions of the monitor plates and the vacuum chamber steps set in; the curve is tilted upward a bit. Near  $n_{\text{cutoff}}$ , the curve starts rising to the free-space radiation value. After about  $n \sim 10^6$ , the resistive part comes mainly from the free-space radiation plus the contribution of the steps. The resonances of the gaps of the laminations of the Lambertsons can still be seen near cutoff frequency while the resonances of the convolutions of the bellows are highly visible. The imaginary part starts off inductively also with  $\sim 50 n^{-1/2}$  ohms due to the resistive walls of the beampipe and the surfaces of the laminations of the Lambertsons. Very soon the contributions of the bellows, monitor plates and vacuum chamber steps set in. The imaginary curve then oscillates from inductive to capacitive and vice versa at the bellow's resonances, and at the same time decays exponentially. Finally, it follows the space-charge curve of the beampipe and is capacitive. For  $E = 1000 \text{ GeV}/c^2$ , because of the smallness of the space-charge contribution, before following the space-charge, the imaginary curve first matches with the inductive free-space radiation curve and vanishes near  $n \sim 10^9$ .

We see that except for very low harmonics ( $n \lesssim 10^2$ ), both the real part and imaginary part of  $Z_n/n$  are less than a few ohms. Thus beam stability can be achieved so far as the Keil-Schnell criterion is concerned. The problem of beam stability at harmonics  $< 10^4$  will be considered elsewhere.

References

1. A. Faltens and L.J. Laslett, Proc. of the 1975 ISABELLE Summer Study, Vol. II, p. 486, Brookhaven National Laboratory
2. A.G. Ruggiero, Proc. of the 1979 Workshop on Beam Current Limitations in Storage Rings, edited by C. Pellegrini, p. 39, Brookhaven National Laboratory
3. J. Schwinger, Phys. Rev. 75, 1912 (1949)
4. A.G. Bonch-Osmolovsky, p. 9-6318, J.I.N.R., Dubna, 1972
5. E. Keil and B. Zotter, Particle Accelerators 3, 11 (1972)
6. A.G. Ruggiero, P. Stolin and V.C. Vaccaro, CERN/ISR-RF-TH/69-7; K.Y. Ng, UPC #148
7. H.G. Hereward, CERN/ISR-DI/75-47
8. M. Sands, PEP-253
9. H.A. Bethe, Phys. Rev. 66, 163 (1944)
10. K.Y. Ng, UPC #149

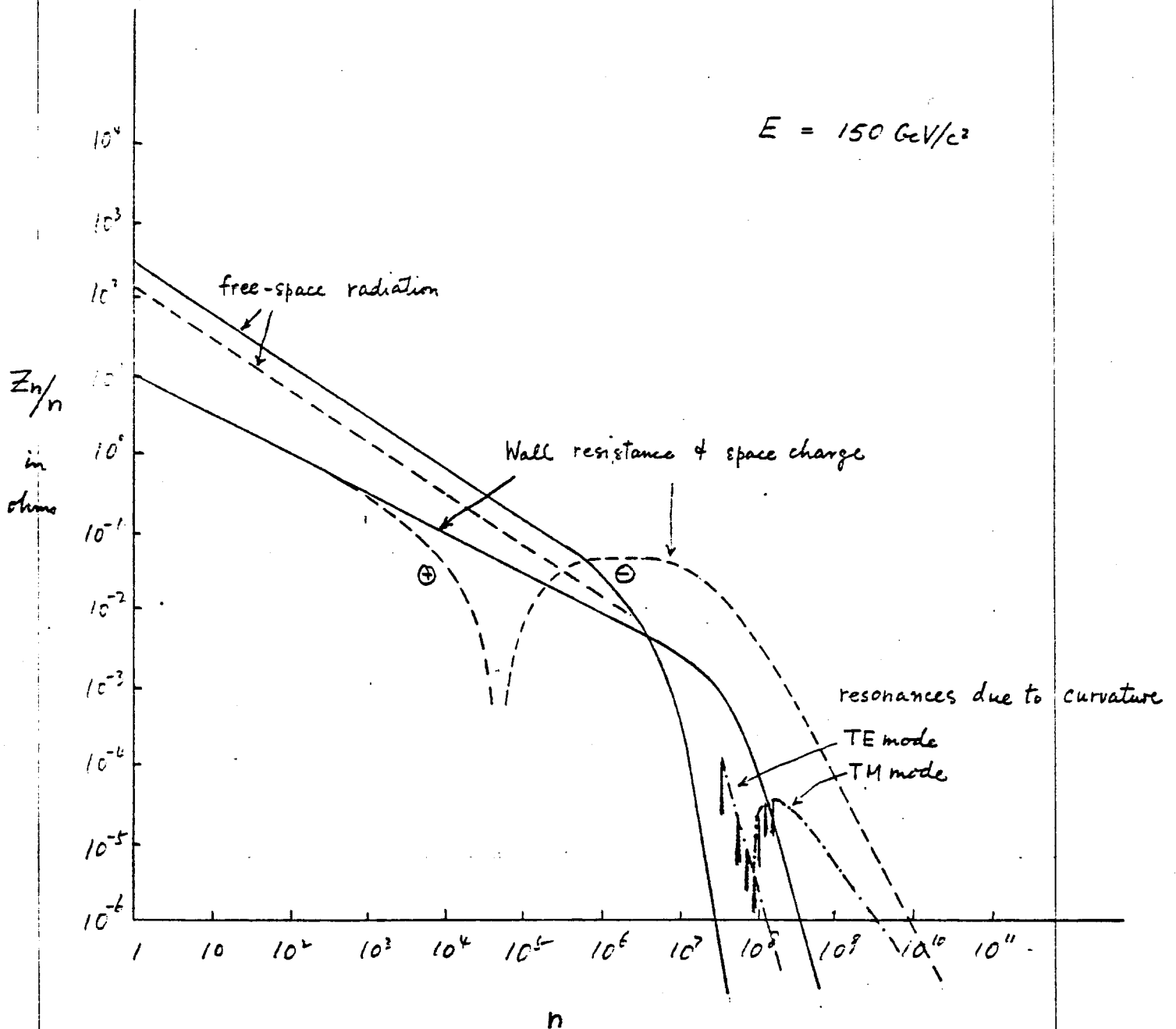


Fig. 1. Wall resistance & space charge contribution at  $150 \text{ GeV}/c^2$ .  $\oplus$  implies inductive and  $\ominus$  capacitive.   
 solid curves are real parts and dashed curves

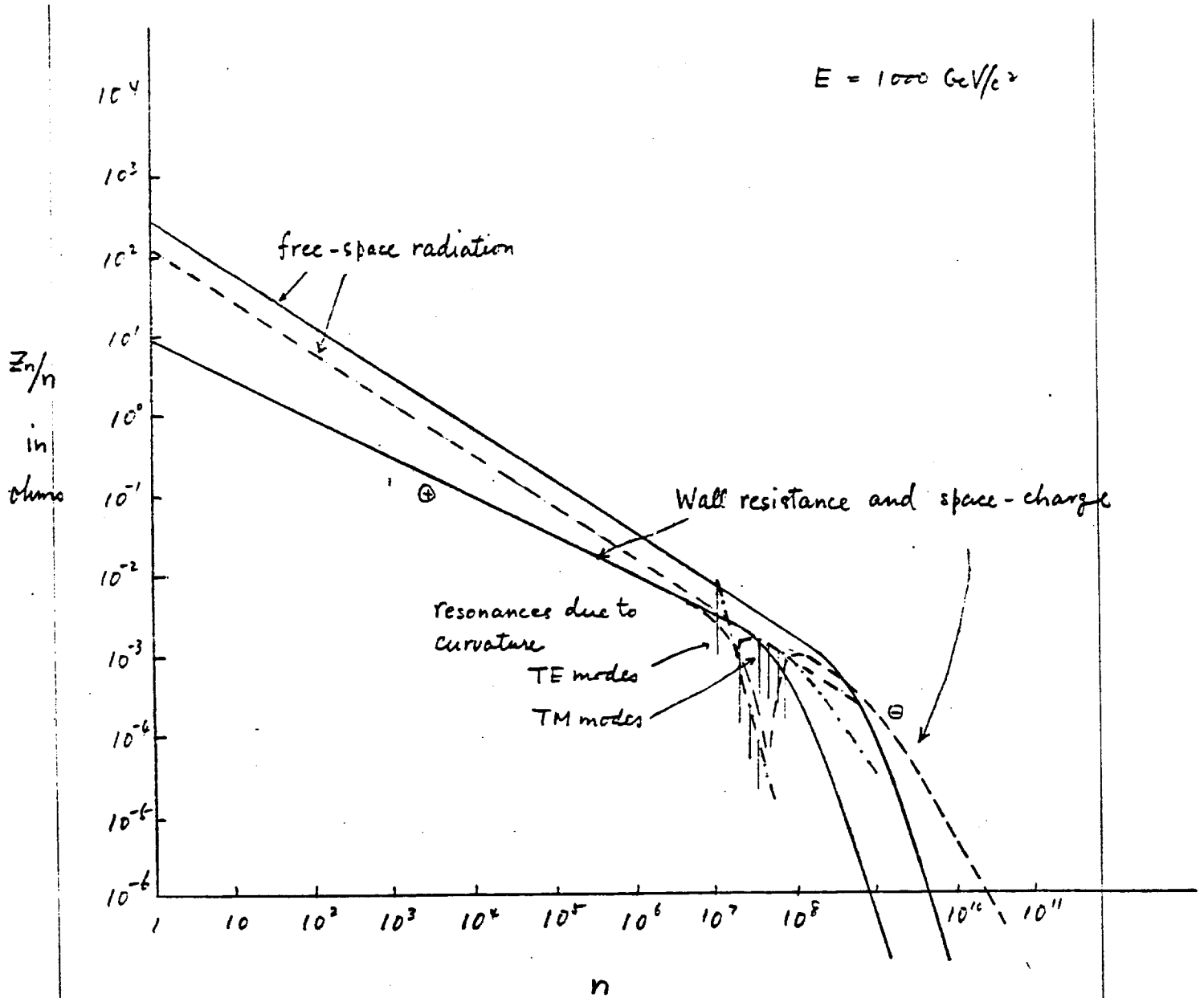


Fig. 2 Wall resistance and space-charge contribution at  $1000 \text{ GeV}/c^2$ .  
 Solid curves are real parts and dashed curves are  
 imaginary parts. ⊕ implies inductive and ⊖  
 capacitive

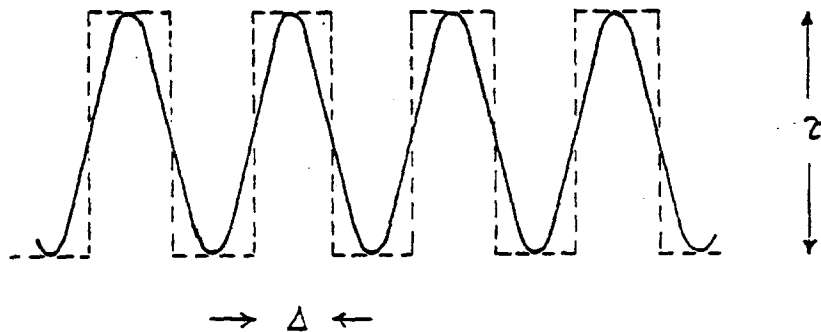


Fig. 3.

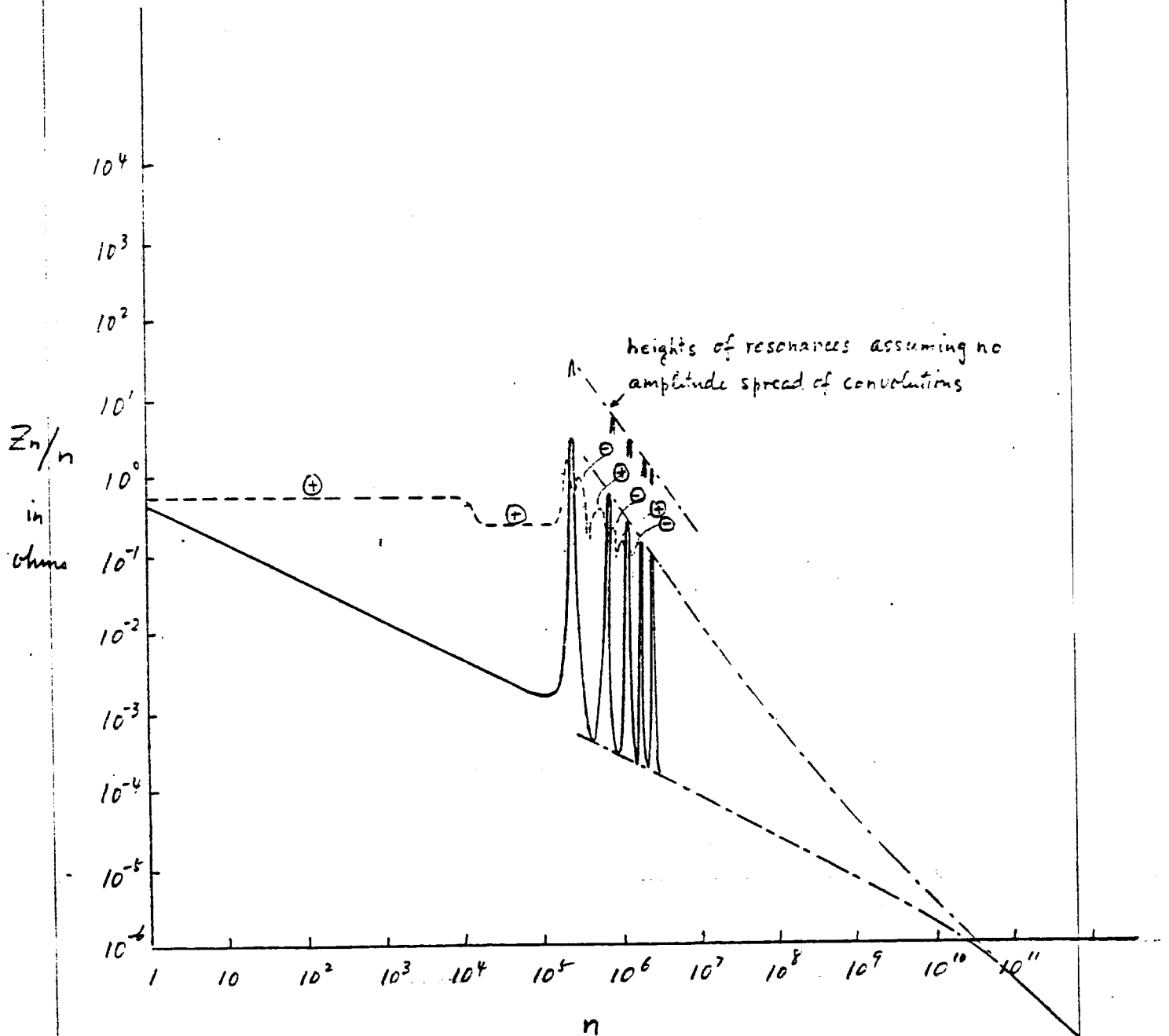


Fig. 4 Contribution of bellows. Solid curve is the real part and dashed curve the imaginary part  
 $\oplus$  implies inductive and  $\ominus$  capacitive

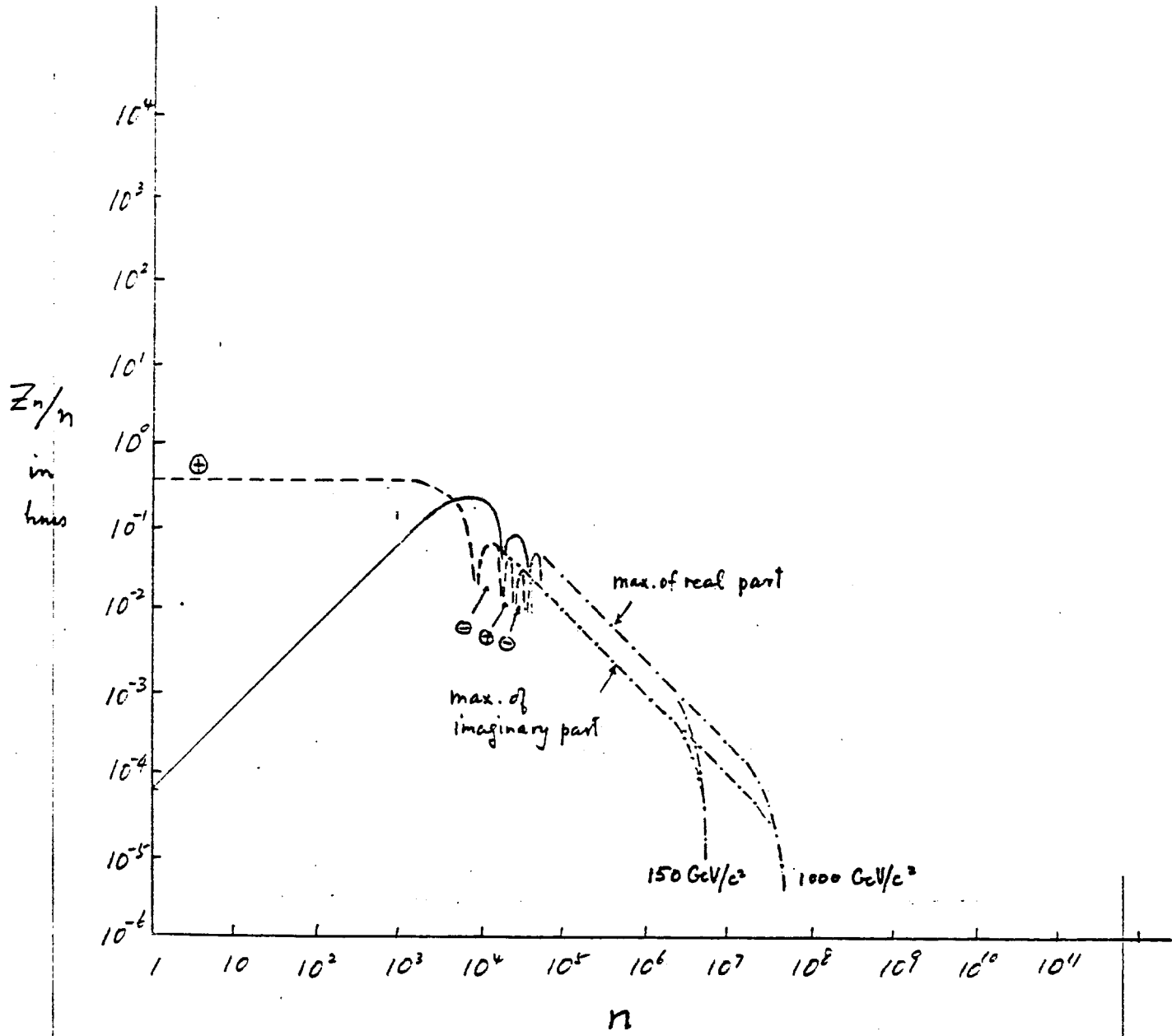


Fig. 5 Contribution of monitor plates. Solid curve is the real part and dashed curve is the imaginary.  $\oplus$  implies inductive and  $\ominus$  capacitive

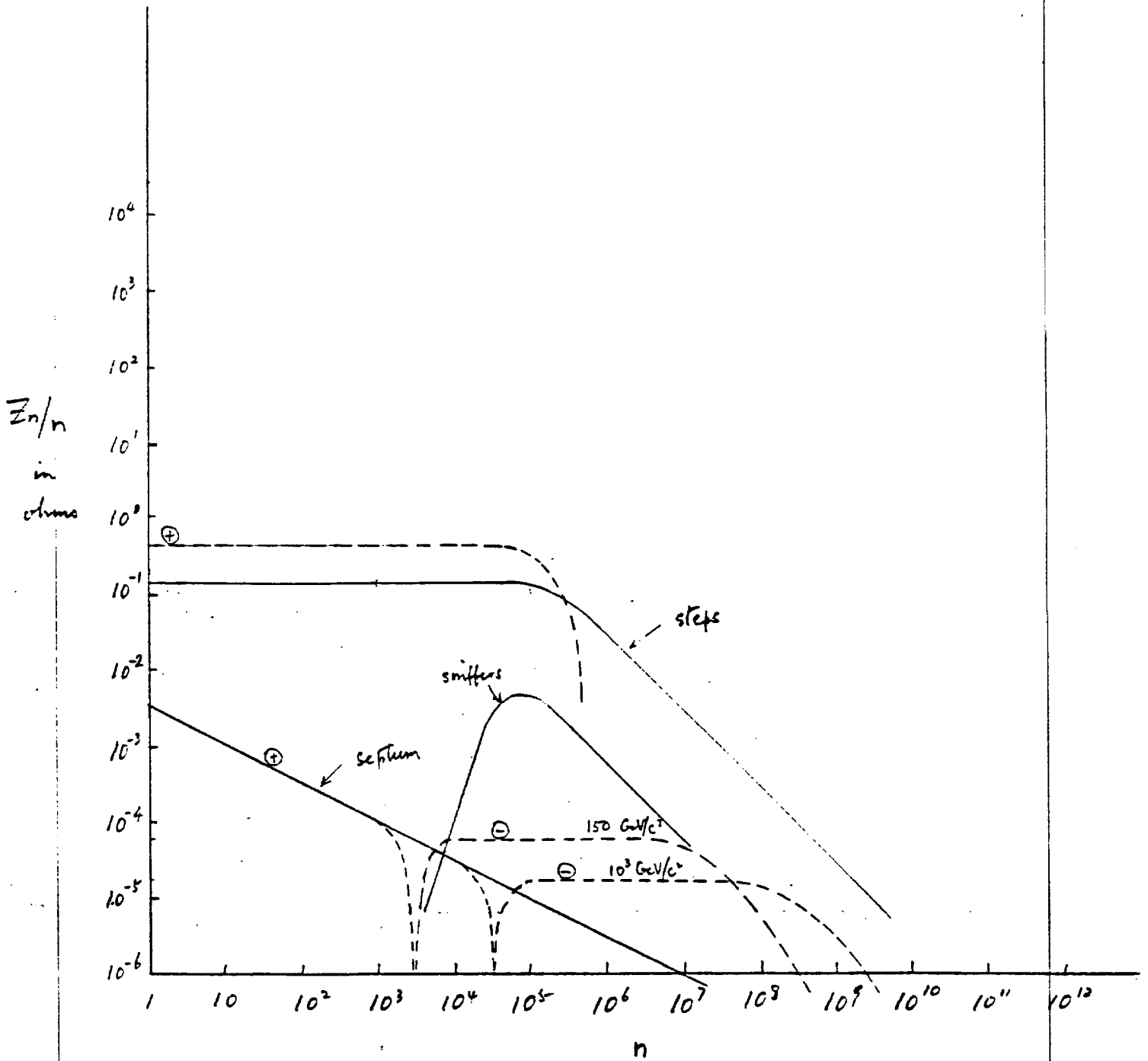


Fig. 6 Contributions of vacuum chamber steps, sniffers and electrostatic septum. Solid curves are real parts and dashed curves imaginary parts.  $\oplus$  implies inductive and  $\ominus$  capacitive.

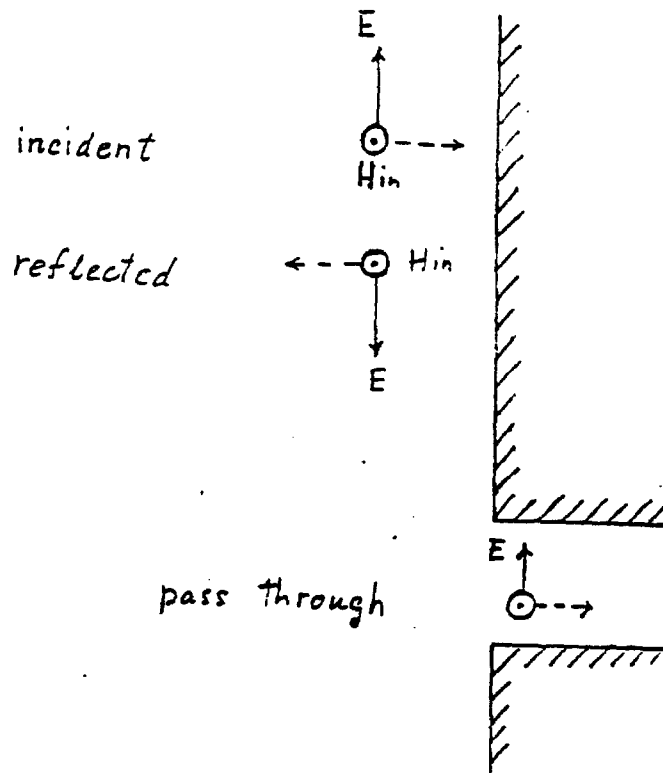


Fig. 7. Radiation at snuffers at high frequencies.

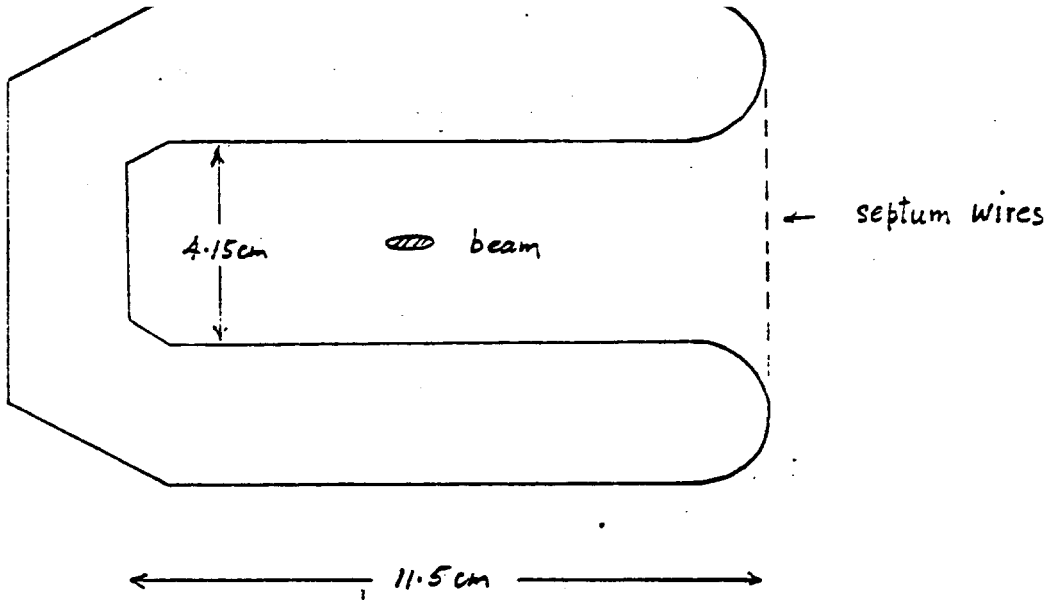


Fig. 8. The electrostatic septum

Table 2

Resonant harmonics for TE modes at injection energy (150 GeV/c<sup>2</sup>):

k=1	k=2	k=3
3.4x10 <sup>7</sup>	5.8x10 <sup>7</sup>	7.1x10 <sup>7</sup> -----
1.6x10 <sup>8</sup>	1.7x10 <sup>8</sup>	1.8x10 <sup>8</sup>
2.9x10 <sup>8</sup>	2.9x10 <sup>8</sup>	-----
-----	-----	

Resonant harmonics for TM modes at injection energy (150 GeV/c<sup>2</sup>):

k=1	k=2	k=3
9.9x10 <sup>7</sup>	1.1x10 <sup>7</sup>	-----
2.3x10 <sup>8</sup>	-----	
-----		



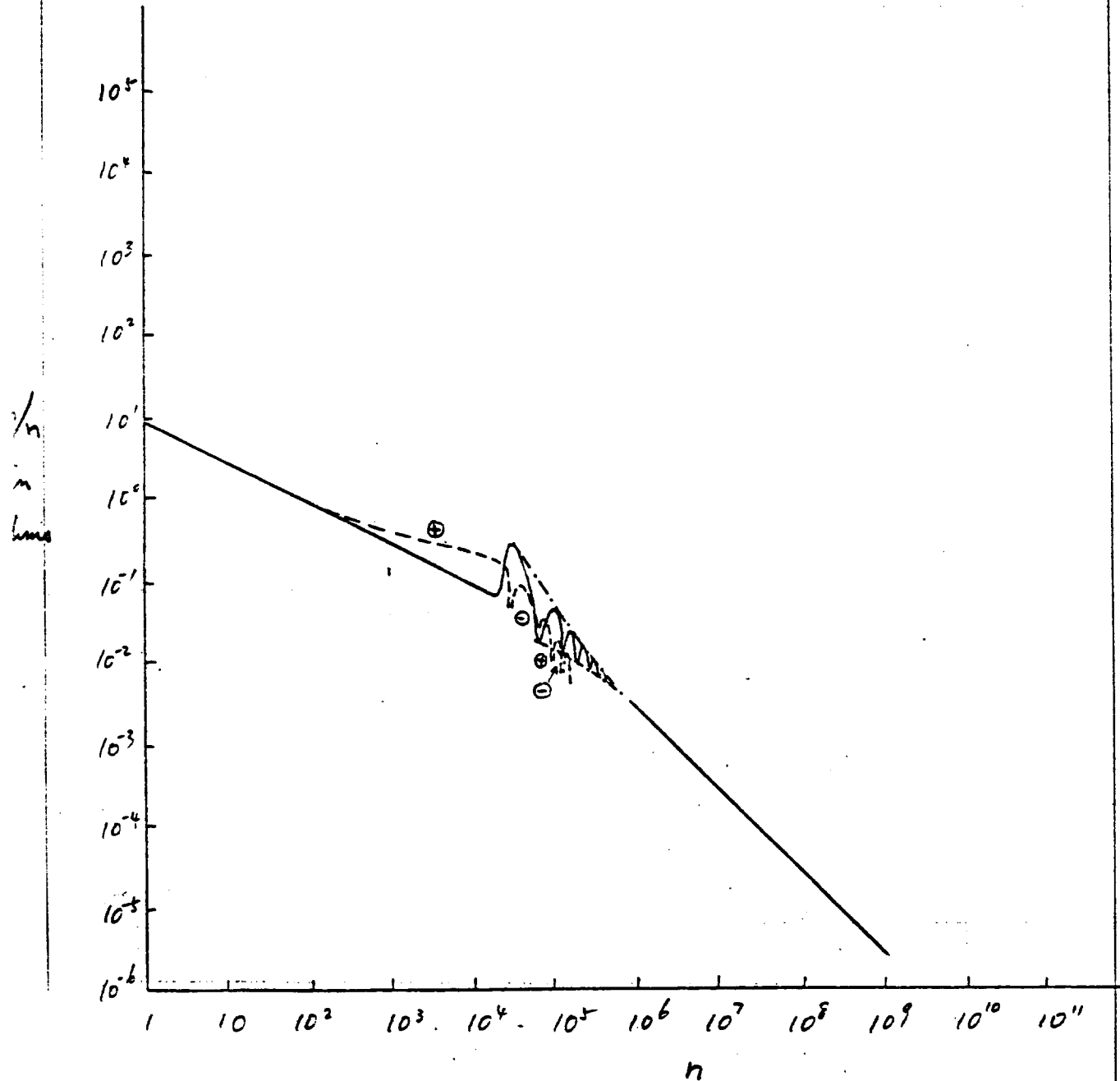


Fig. 10 Contribution of extraction (or injection) Lambertsons. Solid curve is the real part and dashed curve the imaginary part.  $\oplus$  implies inductive and  $\ominus$  capacitive.

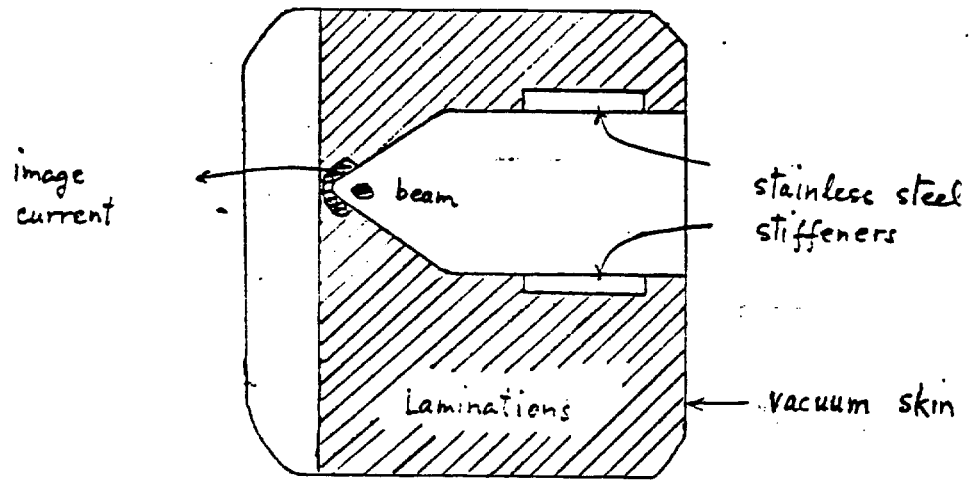


Fig. 9a

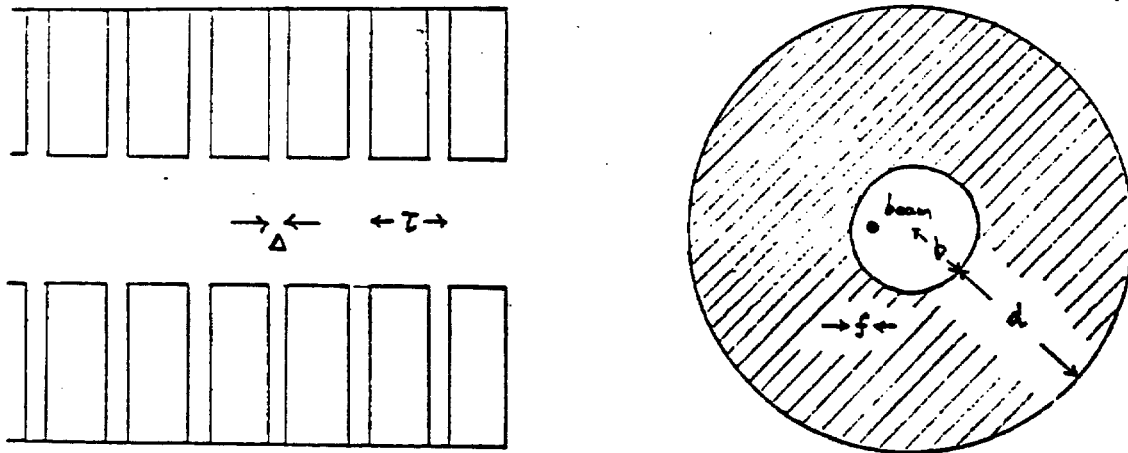


Fig. 9b

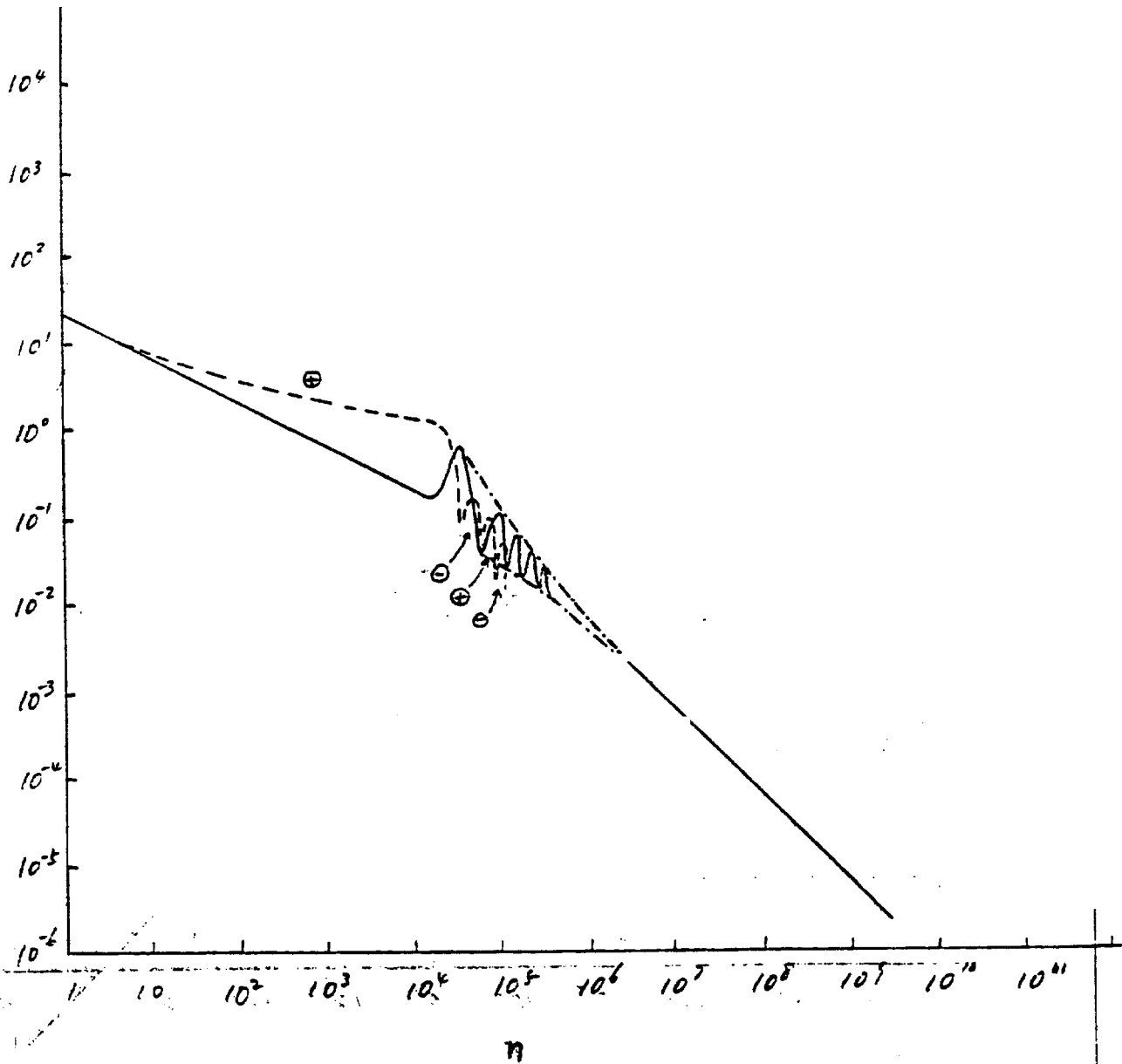


Fig. 12. Contribution of about Lambertsons. Solid curve is the real part and dashed curve the imaginary part  
 $\oplus$  implies inductive and  $\ominus$  capacitive.

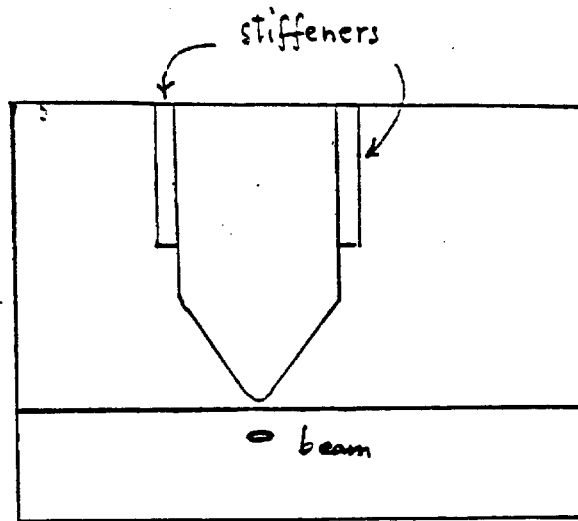


Fig. 11 a

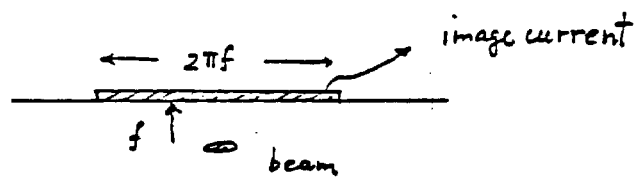


Fig. 11 b.

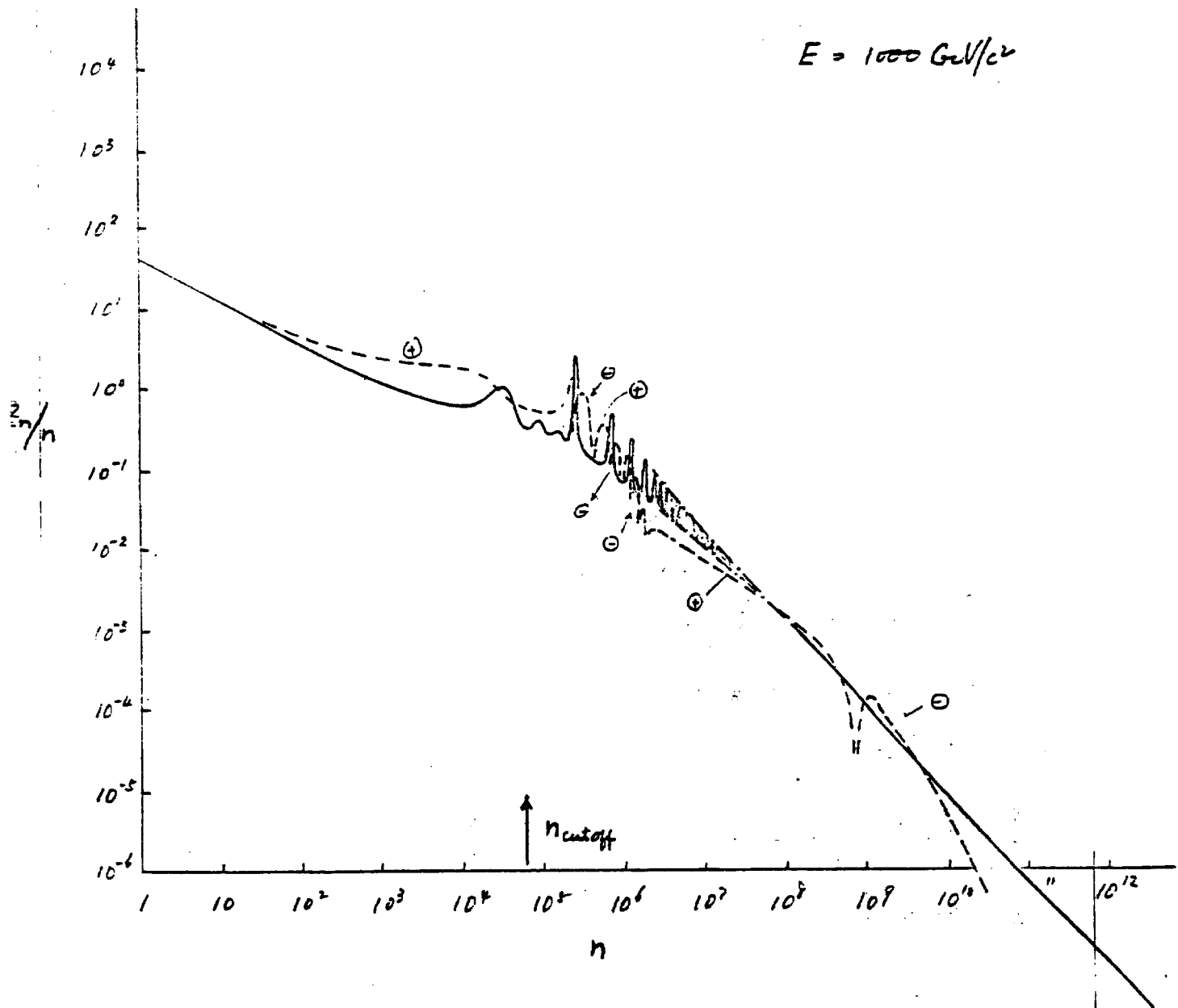


Fig. 14. Sum of all contributions discussed at  $1000 \text{ GeV}/c^2$  except RF cavities. Solid curve is the real part and dashed curve the imaginary part.  $\oplus$  implies inductive and  $\ominus$  capacitive.

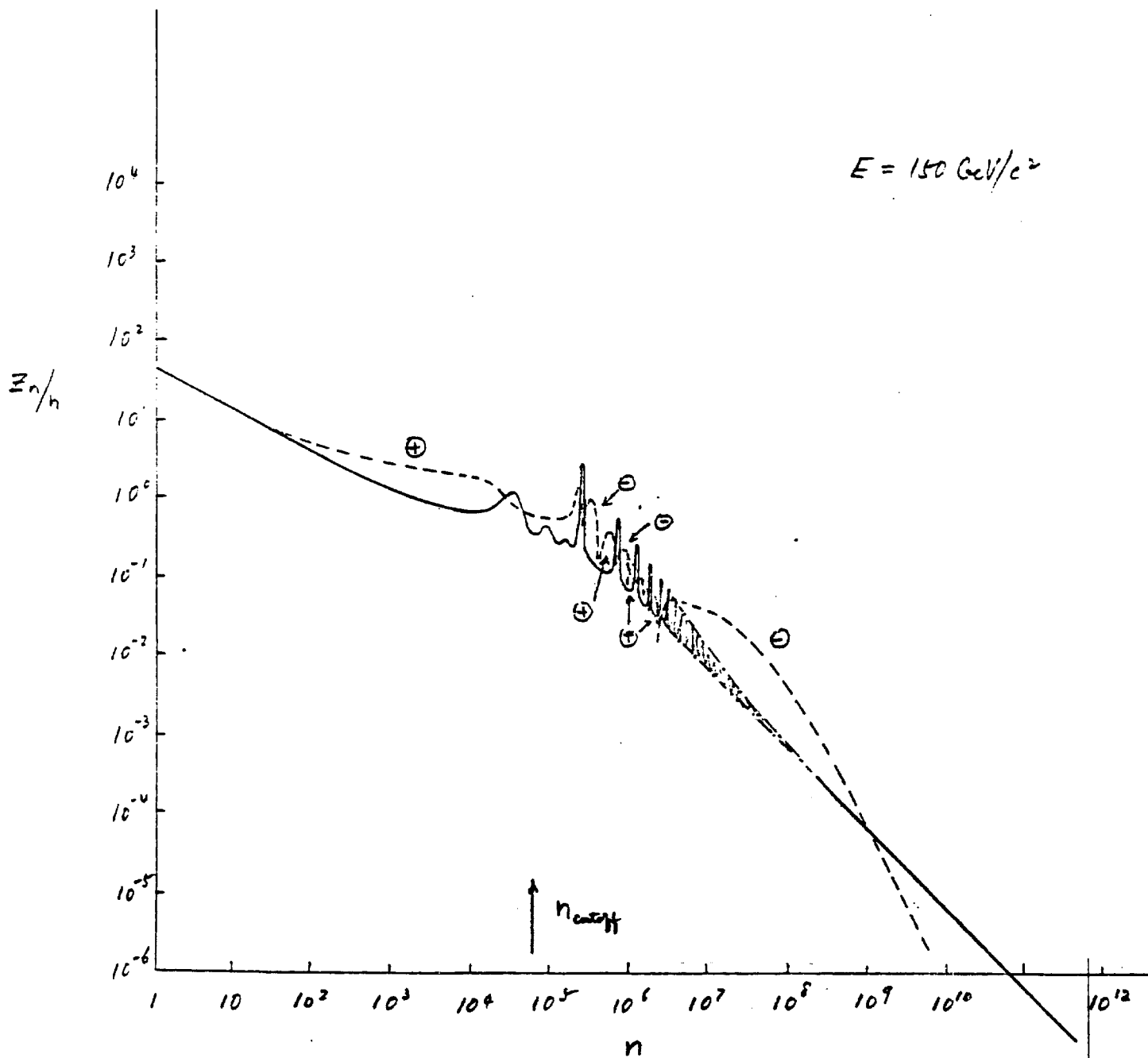


Fig. 13. Sum of all contributions discussed at  $150 \text{ GeV}/c^2$  except RF cavities. Solid curve is the real part and dashed curve the imaginary part.  $\oplus$  implies inductive and  $\ominus$  capacitive.